

INSTITUTO UNIVERSITÁRIO DE LISBOA

October, 2023

Classification of Aortic Stenosis based on AI in MRI Scans
Pedro Miguel Ferreira Viegas Águas
Master's in Integrated Decision Support Systems
Supervisor: PhD João Pedro Afonso Oliveira da Silva, Assistant professor, Iscte-iul
Co- Supervisor: MSc Luís Manuel Nobre de Brito Elvas, Invited Assistant Professor, Iscte-iul



Department of Information Science and Technology
Classification of Aortic Stenosis based on AI in MRI Scans
Pedro Miguel Ferreira Viegas Águas
Master's in Integrated Decision Support Systems
Supervisor: PhD João Pedro Afonso Oliveira da Silva, Assistant professor, Iscte-iul
Co- Supervisor: MSc Luís Manuel Nobre de Brito Elvas, Invited Assistant Professor, Iscte-iul
October, 2023



Pedro Miguel Ferreira Viegas Águas



Acknowledgments

I wish to express my profound appreciation and gratitude to the individuals who have consistently supported me throughout this challenging journey.

First and foremost, I want to thank Professor Luis Elvas for being both my esteemed professor and an amazing friend. I want to thank for the help and patience not just throughout my thesis, but also throughout my two-year Master's degree.

To my mentor, Joao Pedro Oliveira, who successfully guided me in crafting this thesis, passing me his knowledge, criticism and opinions in a manner that I would develop the best research work.

To the Professor João Carlos Ferreira during my Master's, who offered consistent assistance during my Master's program. His guidance, patience, and imparted wisdom significantly enriched my professional and personal growth during my time at lscte.

I want to acknowledge Professor Luís Rosário, our cardiology specialist, for dedicating his time to our meetings, which proved crucial to the development of my research work.

To my family that were worried that I wouldn't finish this task and pressured me at the right times so I would finish, giving me support and inspiration.

I must express my gratitude to my friends, Joana Martins, José Fernandes, and Ana Vieira, who have been there for me since the beginning and have given me strength. Making me see this as an essential step in my career and making this research work look easy. To the days when they challenged me and said I wouldn't finish, and to the days when I needed their help to continue and complete this goal.

To each of you who believed in me and possessed the patience to assist me, I offer my heartfelt gratitude. Your support was pivotal in my successful completion of this work.

With these words, I dedicate this work to all of you with immense pride.

Sincerely,

Pedro Águas

Abstract

Aortic stenosis (AS) stands as a significant cardiovascular ailment necessitating accurate diagnosis for effective patient management. This study introduces an innovative AI-based approach for AS detection in MRI scans. Our research aims to find a robust CNN model combined with computer vision techniques for the classification of AS in MRI, further refined through fine tuning.

We evaluated five CNN models combined with computer vision techniques, where VGG16 model got the best results in our research work, with 95% in recall and 95% in F1-score. In this test four Data Augmentation techniques were implemented including Translation, Rotation, Flip and Brightness, enhancing the model's robustness and generalization, encompassing real-world image variations encountered in clinical settings.

This validation reaffirms the model's clinical applicability, promising streamlined diagnostics while allowing medical professionals to focus on intricate decision-making and personalized care.

In conclusion, our study underscores the potential of Al-driven AS detection in MRI. The merger of transfer learning and data augmentation yields high accuracy rates, validated in real clinical cases, signifying a significant advancement in precise cardiovascular diagnosis.

Keywords: MRI Imaging Techniques; Aortic Disease Classification; Artificial Intelligence; Deep Learning

Resumo

A estenose aórtica (EA) é uma doença cardiovascular significativa, que requer um diagnóstico exato para uma gestão eficaz dos doentes. Este estudo apresenta uma abordagem inovadora baseada em IA para a deteção de EA em exames de RM. A nossa investigação tem como objetivo encontrar um modelo CNN robusto, combinado com técnicas de visão por computador, para a classificação de EA em RM, aperfeiçoado através de *Fine Tuning*.

Avaliámos cinco modelos CNN combinados com técnicas de visão computacional, tendo o modelo VGG16 obtido os melhores resultados no nosso trabalho de investigação, com 95% de *recall* e 95% de *F1-Score*. Neste teste foram implementadas quatro técnicas de *Data Augmentation*, incluindo Translação, Rotação, Inverter e Brilho, aumentando a robustez e a generalização do modelo, abrangendo variações de imagens do mundo real encontradas em ambientes clínicos.

Esta validação reafirma a aplicabilidade clínica do modelo, prometendo diagnósticos simplificados e permitindo que os profissionais médicos se concentrem na tomada de decisões complexas e nos cuidados personalizados.

Em conclusão, nosso estudo ressalta o potencial da deteção de EA orientada por IA em RM. A fusão de aprendizagem por transferência e aumento de dados produz taxas de precisão elevadas, validadas em casos clínicos reais, significando um avanço significativo no diagnóstico cardiovascular preciso.

Palavras-chave: Técnicas de Imagem por RM; Classificação de Doenças da Aorta; Inteligência Artificial; Aprendizagem Profunda

Index

Acknowledgments	lii
Abstract	V
Resumo	vii
List of Figures	ix
List of Tables	x
Glossary	xii
Chapter 1 – Introduction	3
1.2. Objectives	4
1.3. Methodology	5
1.4. Outline of the Dissertation	6
Chapter 2 - State of the Art	7
2.1. Method	7
2.2. Data Extraction	7
2.3. Results	8
2.4. Goals and Outcomes Analysis	10
CHAPTER 3 - CRISP-DM Methodology	13
3.1. Business & Data Understanding	13
3.2. Data Preparation	14
3.3 Modelling	20
CHAPTER 4 - Evaluation and Discussion	23
CHAPTER 5 – Conclusions	29
CHAPTER 6 – Future Work	30
References	31

List of Figures

Figure 1 - Methodology crisp-dm [12]	5
Figure 2 - PRISMA Workflow Diagram	8
Figure 3 - Evolution on eligible studies published by year	8
Figure 4 - Percentage of topic mentioned in the articles	9
Figure 5 - Number of articles including each imaging technique	9
Figure 6 - MRI images without valve	. 15
Figure 7 - MRI of the aortic valve, where the column of images (a) represents the images without A	٩S
and column (b) represents the images that have AS	. 16
Figure 8 - Representation of the rotation technique applied at the default MRI, where (a) represen	ıts
the default MRI and (b) represents the MRI with 90, 180, and 270 rotation degrees, respectively	. 17
Figure 9 - Representation of the translation technique applied at the default MRI, where (a)	
represents the default MRI and (b) represents vertical translation	. 17
Figure 10 - Representation of the flip technique applied at the default MRI, where (a) represents t	he
default MRI and (b) represents the flipped MRIs	. 18
Figure 11 - Representation of the brightness technique applied at the default MRI, where (a)	
represents the default MRI and (b) represents the brighter MRIs.	
Figure 12 - Summarization of the data preparation	. 19
Figure 13 - Percentage of test and train images	. 21
Figure 14 - Developed CNN architecture	. 24
Figure 15 - Model performance: training vs testing	. 25

List of Tables

Table 1 - Keyword Selection	7
Table 2 - Articles by topics	
Tabela 3 - Results of the custom CNN model with the different datasets	24
Table 4 - Results of the models with different Datasets	27

Glossary

AI - Artificial Intelligence

AS - Aortic Stenosis

AVR - Aortic Valve Replacement

BVA - Bicuspid Aortic Valve

CAD - Coronary Artery Disease

CFR - Coronary Flow Reserve

CFVR - Coronary Flow Velocity Reserve

CMR - Cardiac Magnetic Resonance

CMR - Cardiovascular Magnetic Resonance

CNN - Convolutional Neural Networks

CRISP-DM - Cross-Industry Standard Process for Data Mining

CT - Computed Tomography

CTA - Computed Tomography Angiography

CV - Computer Vision

CVD - Cardiovascular Disease

DCNN - Deep Convolutional Neural Network

DL - Deep Learning

FCDL - FC-DenseNet and the level set method

FCN - Fully Convolutional Neural Networks

FN - False Negatives

FP - False Positives

HSM - Hospital Santa Maria

LV - Left Ventricular

MBF - Myocardial Blood Flow

MF - Myocardial Fibroses

ML - Machine Learning

MPI - Myocardial Perfusion Imaging

NR - Normalization Region

PC-MRI - Phase-Contrast Cine Magnetic Resonance Imaging

PD - Pressure Drop

PET - Positron Emission Tomography

PRISMA - Preferred Reporting Items for Systematic Reviews and Meta-Analyses

PVS - Prosthetic Valve Size

RDIR - Reverse Double Inversion-Recovery

ROI - Region of Interest

RQ - Research Question

RV - Right Ventricular

TAVR - Transcatheter Aortic Valve Replacement

TN -True Negatives

TP - True Positives

UL - U-Net + level set

WoSCC - Web of Science Core Collection

Chapter 1 – Introduction

Cardiovascular disease (CVD) is the leading cause of death worldwide and has been increasing gradually over time [1], [2]. According to the World Health Organization (WHO), CVDs are the leading cause of death globally [1]. In 2019, an estimated 17.9 million people died from CVDs, accounting for 32% of all global deaths [1]. Of these deaths, 85% were due to heart attack and stroke [1]. Over three quarters of CVD deaths take place in low and middle-income countries [1].

Aortic Stenosis (AS) is a CVD that represents a form of heart valve disease primarily affecting the left ventricle, where the valve gradually becomes calcified. The calcification process leads to valve thickening, narrowing, and weakening, impeding its full opening. Consequently, blood flow through the aortic valve diminishes, giving rise to complications such as blood clots, strokes, heart failure, and even cardiac rhythm irregularities. The prevalence of AS is on the rise, driven not only by an aging population, with approximately 6% to 12.4% of elderly individuals afflicted by this condition [3], [4], but also exacerbated by the emergence of the COVID-19 pandemic in 2019.

The introduction of COVID-19 has brought with it an abundance of issues, most notably a significant problem with accessing hospital-based cardiovascular care, which has resulted in a drop in necessary cardiovascular diagnostic tests. As a result, fewer patients received timely diagnoses. This situation was further aggravated by the pandemic's effect on myocardial health, which manifested as larger infarct sizes, more widespread microvascular blockage, a greater frequency of intramyocardial bleeding, and a higher prevalence of AS disease [5]. Remarkably, patients with AS were discovered to be a large group contributing to COVID-19-related mortality [6].

In the context of these challenges, Magnetic Resonance Imaging (MRI), among other imaging modalities, has emerged as a fundamental technology. When compared to standard echocardiographic investigations, MRI has showed superiority in terms of repeatability and accuracy in detecting clinically relevant changes in Left Ventricular (LV) size and function [7].

To overcome the increase of AS disease, applying artificial intelligence (AI) to analyze cardiac MRIs has demonstrated a drastic improvement in the ability to detect early signs or future risk [8]. Using this solution would not only improve patient care, but it will implement better early strategies for treatment, achieving better outcomes [8]. Convolution Neural Networks (CNN) were introduced as deep-learning algorithms, allowing accurate and fully automated image analysis. These AI-based analyses are considered feasible, reproducible, and demonstrate valuable prognostic in patients with AS disease, saving time and making clinical routine easier [7]. The fundamental benefit of CNNs over more traditional Machine Learning (ML) algorithms is that, during training, feature extraction is handled automatically without the need for pre-existing notions about what features to extract. This

means if you have a ML algorithm to train, it needs the images classified with the different features [9]. On the other hand, a Deep Learning (DL) algorithm will learn the features automatically without any a priori definition [9].

Consequently, this research investigates the application of AI for automatic classification of MRIs of patients suffering from AS. By reducing the workload of healthcare professionals, we aim to mitigate the disease's impact, reduce resource allocation, and minimize healthcare expenses.

In the ever-evolving landscape of healthcare and medical research, the collaboration between academic institutions and hospitals plays an important role in advancing our understanding of complex medical phenomena, improving patient care, and driving innovation in the field [10]. This master's thesis represents the culmination of a collaborative effort between Iscte and Hospital Santa Maria (HSM), aimed at contributing to the forefront of healthcare research.

The overarching objective of this research endeavor is to explore, analyze, and contribute to the multifaceted world of healthcare through a lens that fuses theory with practice. By bridging the gap between academia and clinical practice, we aim to address critical questions, innovate new methodologies, and unearth solutions that hold the potential to transform patient outcomes and enhance the quality of healthcare delivery.

1.2. Objectives

This study aims to find a robust CNN model combined with computer vision techniques for the classification of AS in MRI, originating the Research Question (RQ) "How can we effectively use AI to automatically classify MRI scans from patients suffering from AS?".

In order to answer the RQ and classify MRI images a CNN model combined with computer vision techniques needs to be implemented and tested so we can successfully distinguish between cases with AS and those without. This classification task involves the binary decision of whether or not aortic valve stenosis is present.

To accomplish our objectives and address our research question, we have adopted the CRISP-DM (Cross-Industry Standard Process for Data Mining) methodology [11], for image data. This methodology guides us through various stages, such as data selection and collection, preprocessing, feature extraction, model development, training, validation, evaluation, and deployment, to achieve specific research goals.

Throughout our research, we should emphasize the clinical significance of the work and how it can reduce the medical workload when classifying the MRIs, a condition that has significant implications for patients' cardiovascular health.

1.3. Methodology

The CRISP-DM, see Figure 1, is a framework for data mining and analysis initiatives. CRISP-DM offers a disciplined and systematic approach to resolving complicated issues in the field of computer vision, enabling a full and effective analysis of the data and its properties. This methodology, which covers the complete data mining process from start to finish, is especially well-suited for computer vision users [11]. This includes describing the issue, collecting and understanding the data, putting the data in order, cleaning it, creating and validating models, and using the models to address the issue at hand.

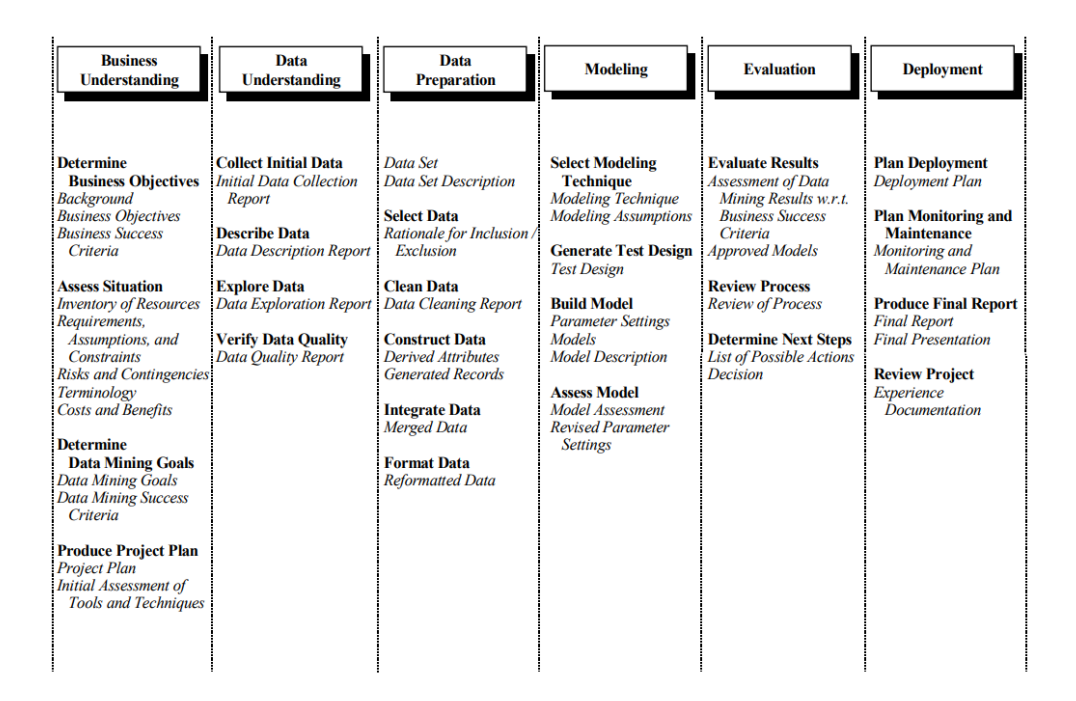


Figure 1 - Methodology crisp-dm [12]

This methodology has 6 phases, each one focusing on different tasks as shown next:

- 1. Business understanding: To understand the problem we are studying.
- **2. Data understanding:** To understand with which images we are working with and what methods should be used to develop the work.
- **3. Data preparation:** Prepare and filter data to create a reliable Dataset to train and test the models that can be trained and tested.
- **4. Modeling:** Investigate and explain the model used.
- 5. Evaluation: Evaluate the model and analyze the output of each model.
- **6. Deployment:** Our deployment phase is represented by this master thesis and an article that has been submitted and that we are waiting for review.

1.4. Outline of the Dissertation

After the goals and strategy have been set, there will be six chapters, including the Introduction. In the following chapters were included:

Chapter 2: A literature review on the state-of-the-art of calcium scoring and calcification from MRI images, using computer vision, and explanation and task from PRISMA (Preferred Reporting Items for Systematic Reviews and Meta-Analyses) method.

Chapter 3: Following the Methodology CRISP-DM, we create the Dataset, use Data Augmentation techniques and explain the models used in the research.

Chapter 4: Result and Discussion.

Chapter 5: Conclusions and Future Work, along with a discussion of the research's findings.

Chapter 2 - State of the Art

2.1. Method

Based on the PRISMA approach, this systematic review statement was developed to assist authors in better reporting systematic reviews and meta-analyses [13]. Although PRISMA can also be used as a foundation for presenting systematic reviews of other research forms and notable evaluations of therapies, it has been mostly used to report randomized trials.

2.2. Data Extraction

The search was done in Scopus and Web of Science Core Collection (WoSCC) databases performed in 2023. To make this search, a query was created with an interception between the columns with a limitation, only journal papers, articles, and reviews from the last 5 years, and written in English, as shown in Table 1.

Table 1 - Keyword Selection

Concept	Population	Context	Limitations
"Artificial Intelligence"	"Magnetic Resonance	"Aortic stenosis"	Last 5 years
"Computer Vision"	Imaging"	"Calcium Score"	Only journal papers,
"Deep Learning"	"MRI"	"Aortic Calcification"	articles, reviews and
"Image Processing"			written in English
530,296 Documents			
25,876 Documents			
63 Documents			

2.3. Results

After applying the query to both WoS and Scopus databases, 63 documents were found. However, by removing duplicates and excluding some articles without the information needed, only 40 papers were used in this research study. These steps are shown in Figure 2.

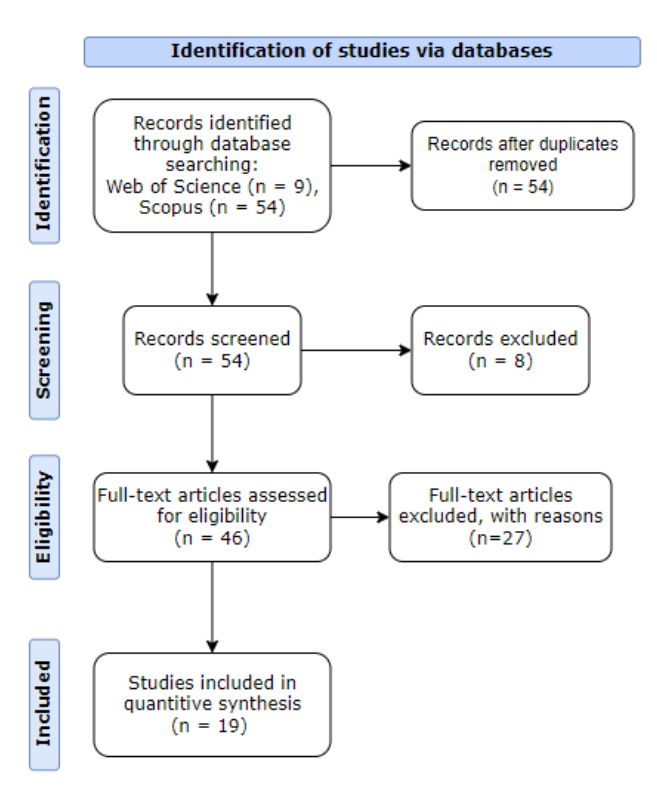


Figure 2 - PRISMA Workflow Diagram

Considering AI is becoming a more used technology for medical care, researchers are making more studies, making a relevance growth in research work published each year, Figure 3.

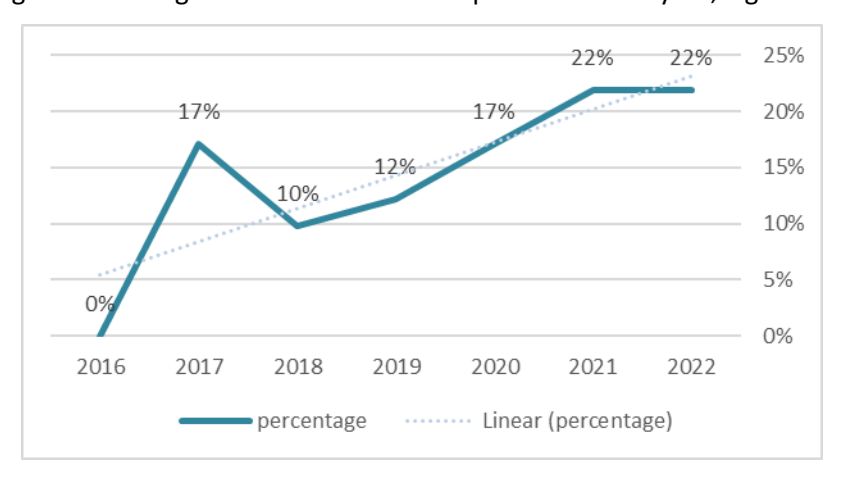


Figure 3 - Evolution on eligible studies published by year

After reading the selected articles for this research work and analyzing the topics studied in it, Aortic Disease, MRI, and AI are the most common topics, as shown in Figure 4.

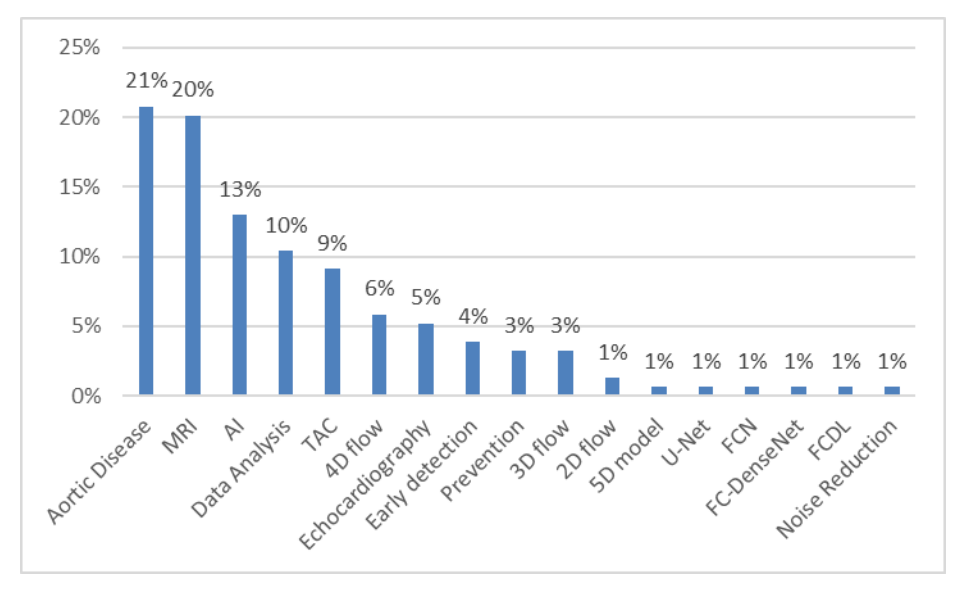


Figure 4 - Percentage of topic mentioned in the articles

As shown in Figure 5, the majority of articles discuss MRI as an imaging technique, followed by CT-scans and echocardiography.

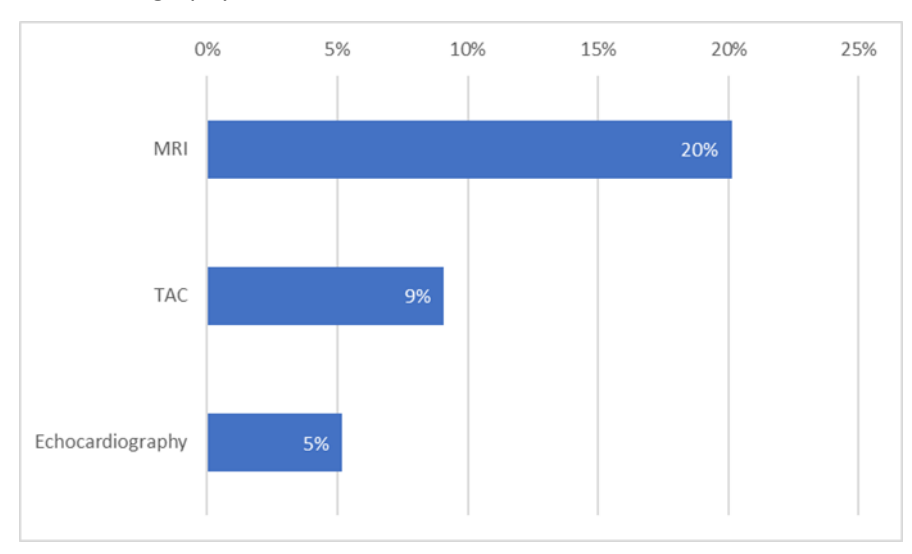


Figure 5 - Number of articles including each imaging technique

2.4. Goals and Outcomes Analysis

Knowing that the main objective of this research work is to identify aortic stenosis disease by applying AI on cardiac images, a table with a description of the main areas addressed in the papers is summarized in Table 2.

Table 2 - Articles by topics

Topic	References		%
Τορις			Doc
Aortic Disease/Aortic	[3]–[5], [7], [9], [14]–[40]		21%
Stenosis			21/0
MRI	[3]–[5], [8], [9], [14]–[16], [20]–[38], [41]–[44]	31	20%
Artificial Intelligence	[3], [5], [8], [9], [16], [18], [19], [23], [25], [31], [35],	20	13%
Artificial intelligence	[37], [40], [42], [45]–[50]	20	1370
Tomography Scan	[8], [9], [16], [17], [19], [22], [23], [26], [28], [29], [39],	14	9%
Tomography Scan	[41], [43], [45]	17	370
Echocardiography	[3], [8], [9], [26], [32], [39], [40], [43]	8	5%
Early Detection/	[7], [8], [14], [18], [24], [25], [51]	7	4%
Prevention	[,],[0],[±+],[±0],[±+],[5+],[5+]	,	770

In the field of cardiovascular imaging, the application of AI has led to significant advancements, fundamentally changing the way cardiac diseases are detected and diagnosed [3,6,13,14,18,20,26,32,36,38,42–44]. This literature review provides a comprehensive overview of key developments in this dynamic domain.

Al has proven effective in the classification of aortic calcification using MRI, consistently achieving remarkable accuracy rates ranging from 90% to 93% [19]. However, these authors, when discussing the outcomes of applying AI to aortic calcification, do not emphasize the metric of recall, which is particularly crucial in health cases. For instance, if we have 100 cases and aim to identify those with a specific condition, such as cancer, a scenario where the algorithm classifies everyone as healthy could result in an accuracy of 99%. However, the recall in this case would be 0%, highlighting the importance of considering recall in medical contexts.

All applications, as discussed in [8], hold substantial promise for early detection of cardiovascular risk factors and timely interventions. Extensive literature searches, as evidenced in [23], have unearthed a growing body of studies leveraging All across MRI and CT modalities. These studies encompass diverse applications, from coronary calcium scoring to prognostic assessments for coronary artery disease, signifying Al's potential to transform cardiac imaging for screening and monitoring. In

this study, the researchers discuss the scarcity of datasets and medical images for AI applications but overlook the potential of data augmentation in addressing this issue. Failure to explore data augmentation may limit the model's ability to generalize from training data to real-world environments.

Furthermore, review [5] confirms an increase in research in this area, particularly the application of artificial intelligence in imaging patients with valvular heart disease. This method of operation would allow for systematic screening for coronary artery disease as well as continued monitoring of patients who have been diagnosed with coronary artery disease [47].

According to [25], ML techniques, particularly U-Net architectures, have rapidly advanced the evaluation of aortic diseases, revolutionizing aortic segmentation and showing promise in monitoring aortic aneurysm sizes. As mentioned in this article [19], it is underscored how deep learning applied to MRI enhances image quality, automates analysis, and enhances disease detection and prognosis [9]. Moreover, [49] proposes a deep convolutional neural network (DCNN) based on ResNet50 and uses fine-tuning to train the model for object identification.

The authors of [45] developed a densely connected convolutional network (ASTRO-X) to diagnose cardioembolic stroke using chest radiographs, with a good and plausible classification performance of 91% classified as non-cardiac stroke, demonstrating that transfer learning is an effective strategy. Another paper [40] used the Chan–Vese algorithm, with extra techniques providing more emphasis on the illumination of region of interest (ROI), obtaining accurate detection of the LV chamber to diagnose the volume variations for aortic stenosis and detection of heart failure cases. Motion correction was used to obtain better results and image quality in [16]. Reference [42] proposed a fully automatic RV segmentation method that combines the FC-DenseNet and the level set method (FCDL), making per-pixel semantic inference with ground truth, for smoothing and converging contours to improve accuracy. This research faces a data limitation, comprising only 45 cases. To overcome this constraint, the researchers employed data augmentation techniques to enrich their dataset. Furthermore, the same research indicates that the FCDL method outperforms the U-Net + level set (UL), indicating that the FCDL method is an efficient and suitable solution to RV segmentation. In [35], a three-dimensional ResNet with noise reduction was implemented for MRI, achieving 92% F1-score and 97% recall.

Following the research from [3], echocardiography was the primary technique for evaluating aortic disease. However, due to image quality limitations and valve geometry deviations, MRI has gained prominence. To address these challenges, [50] introduces a fully automated machine learning approach, eliminating the need for manual border delineation.

In conclusion, our comprehensive literature review reveals a scarcity of articles and research dedicated to the application of AI in the context of MRI. This lack of prior studies highlights the

promising nature of our research in this field. Al integration into cardiovascular imaging represents a transformative era characterized by heightened accuracy, early disease detection, and advanced image analysis capabilities [48]. Moreover, a common challenge among researchers is the acknowledgment of limited data access. To address this issue, some studies overcome the challenge by employing strategies such as data augmentation and transfer learning. These innovations hold immense promise for the diagnosis and monitoring of a broad spectrum of cardiovascular conditions [48].

CHAPTER 3 - CRISP-DM Methodology

This research work aims to classify heart MRI by identifying calcification on the aortic valve. The CRISP-DM Methodology, Figure 1, guided this research work, beginning with data preparation and ending in the Deployment stage. The following sections will go into much greater detail.

3.1. Business & Data Understanding

In this chapter, we dive into the foundational aspects of our data, to understand better the data we are working with. The data utilized was sourced from Hospital Santa Maria (HSM) and predominantly comprised medical images. Our access to this extensive dataset, containing data from 512,764 patients, was facilitated through our collaboration with the aimhealth project [52]. Furthermore, we ensured the requisite documentation was in place. This included a comprehensive data dictionary, authorization from the CHULN services spanning Cardiology, Intensive Care Medicine, and the Respiratory Intensive Care Unit. Additionally, we acquired the Curriculum Vitae of the respective physicians overseeing the data. In a commitment to data integrity and security, all personnel with access to the data signed a declaration of honor, affirming their adherence to General Data Protection Regulation (GDPR) regulations. These regulations encompassed safeguarding sensitive information, specifying authorized personnel, defining data retention periods, establishing data disposal procedures, and preventing unauthorized utilization in other research contexts without explicit consent, adhering to the principles outlined in both the Declaration of Helsinki and the Oviedo Convention [53].

Upon successfully navigating the bureaucratic tasks, we received access to two data repositories, where (1) a structured database contained an abundance of reports, patient information, medical procedures, medication records, precautions, schedules, as well as other pertinent data, and (2) a vast repository of medical images capturing various diseases, including Aortic Stenosis, COVID-19, pneumonias, prosthesis-related cases, and fractures. Regrettably, none of these images were labeled. Given our research focus on evaluating MRIs of AS patients, we needed to separate what was relevant from what would be considered useless to our research objectives. This division allowed us to correlate the database with our dataset, making it easier to retrieve relevant information for our study.

In the course of analyzing the medical images supplied by HSM, we observed that they were stored as DICOM files [54]. These files contain essential image metadata, including details such as size, dimensions, bit depth, modality, and parameters related to image capture equipment. Each piece of information is represented by a specific tag, enabling us to apply filters based on patient ID, image type (MRI, CT-Scan, Echo), orientation, and other relevant criteria.

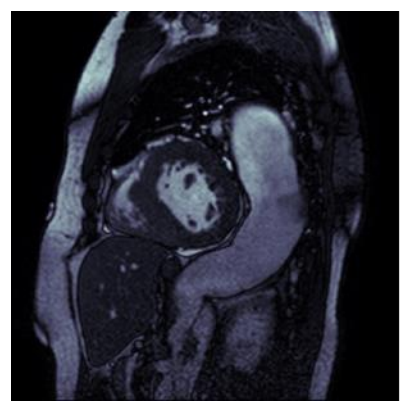
Furthermore, we established a crucial association between the "Patient" and "Diagnoses" tables within the structured database. This association was established through a unique "ID" linked to each diagnosis, which corresponded to the "Patient ID." This strategic linkage allowed us to selectively acquire data pertaining to patients directly relevant to our research, streamlining the process of filtering the MRIs essential for our investigation.

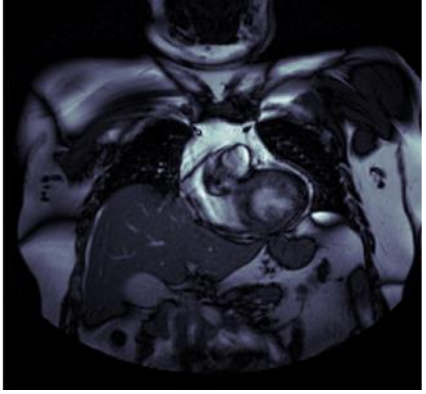
3.2. Data Preparation

In our quest to access a diverse range of medical images, our aim was to analyze only MRIs of patients suffering from Aortic Stenosis.

Our first task was to go through the large image pool and isolate those that were relevant to our research. To accomplish this, we conducted a filtering process on each image in the dataset, selecting only MRI scans that show the heart. This filtering was done based on the metadata contained within each DICOM file, which offers important information about the image data. In our initial filtering step, we selected images that (1) had the 'MRI' image type, represented by the tag (0008,0060) since this tag stores the type of the data originally acquired (for example, CT-scans, MRIs, Audio...) and by (2) the images associated with "heart" examinations using the tag (0018, 0015) representing the "Body Part examined". This selection was necessary as our study primarily focused on heart MRIs. After filtering we got 20,167 heart MRIs, but with multiple diseases outside of the scope of this work. Given the wide variety of diseases, the selected images (MRIs) still went through another filter whereby using a SQL query we have filtered only by the patients that were diagnosed with AS, from the database HSM provided for us. To achieve this filtering, we had to get the IDs of each patient from the selected MRIs to get the diagnosis associated with each image. After this complex task, we ended up with 9,787 MRIs from 24 patients that were diagnosed with AS. However, our endeavor to obtain images specifically related to Aortic Stenosis proved to be challenging due to both the complexity of medical knowledge required and the sheer volume of images involved.

To obtain the finals MRIs that are relevant to the final dataset we had two aspects: first, a considerable portion of the acquired images could not be employed due to their inability to reveal the aortic valve, as demonstrated in Figure 6.





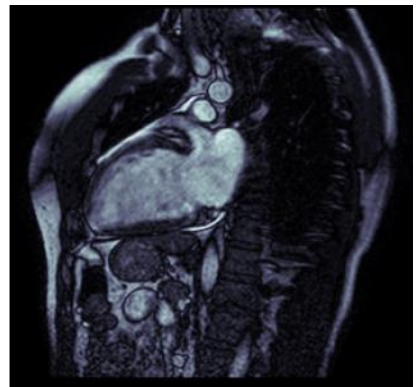


Figure 6 - MRI images without valve

To surpass this challenge, numerous meetings and discussions were held with the cardiology specialist. These meetings were dedicated to imparting knowledge and carefully analyzing each image to determine if it was suitability for our study. Regrettably, this meticulous selection process culminated in a significantly reduced dataset, with only 91 images with AS of the 9,787 MRIs from the last selection, alongside 8 images that were diagnosed without AS. To emphasize the gravity of the situation, it is critical to recognize that a significant amount of time and effort was put into the selection process. Dreadfully, a mere 1% of the initially acquired images found utility in our research. Furthermore, this selection process inadvertently resulted in an imbalanced dataset, adding yet another layer of complexity to our research endeavor. This issue extends beyond our research, potentially affecting others navigating similar paths in the pursuit of medical image analysis.

To compensate for the fact that our dataset was too unbalanced, preventing our model from achieving its full potential and producing the expected outcomes, we introduced a new benchmark dataset, which was also used by the authors in [55]. Subsequently, after finishing and adding the new images to the dataset, the cardiology specialist verified the images to ensure the dataset's reliability.

This way, our Data Preparation was completed, having 111 MRI images without Aortic Stenosis and 91 MRI images with Aortic Stenosis. In Figure 7, we can see some examples of MRI images with and without Aortic Stenosis.

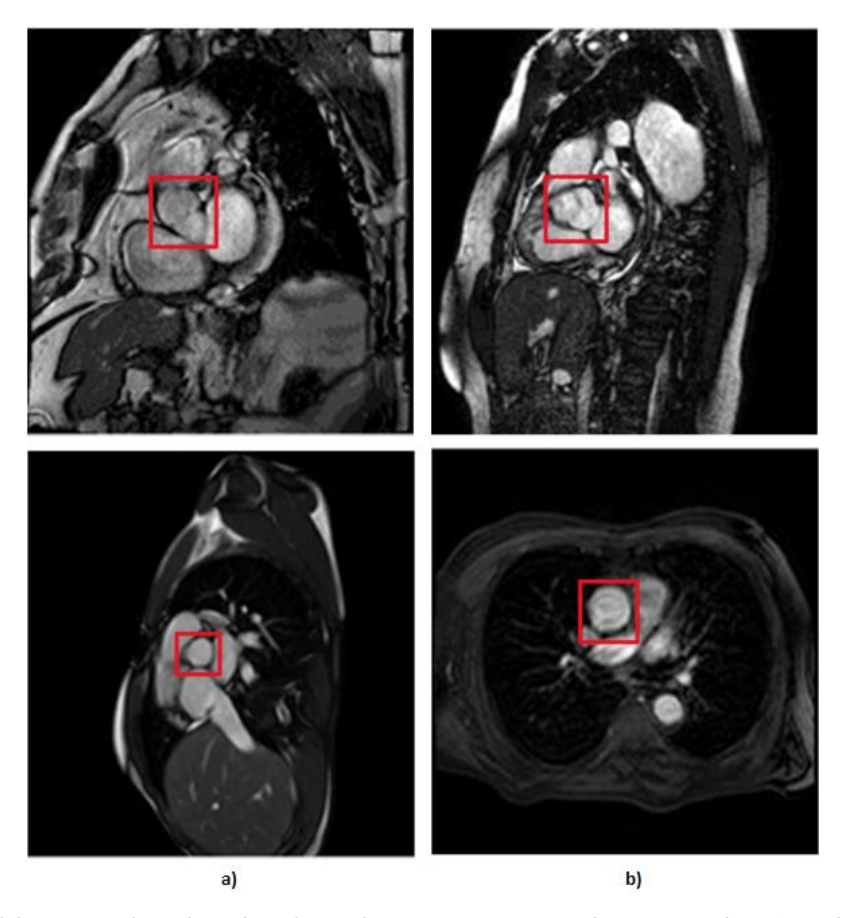


Figure 7 - MRI of the aortic valve, where the column of images (a) represents the images without AS and column (b) represents the images that have AS

With a small dataset of 202 images, including 91 images of AS and 111 images without AS, it is clear that the limitations of the dataset size may prevent this study from achieving the intended research results.

Recognizing the limitations of our small dataset, and to improve its resilience we used data augmentation. With this method we employed four augmentation procedures, each of which aims to create more diverse images without compromising realism in order to improve the final results, where:

(1) We used rotational augmentation to rotate photos at 90, 180, and 270-degree angles, depicted in Figure 8. This geometric modification not only increased the size of our dataset by 3 times, but it also created useful variations in orientation, increasing the information available to our models. We only intended to spin the MRIs at four angles because rotating an MRI to a random degree between those mentioned above would not be realistic, because the patient is not in a 15 degree position during the exam, for example. This creates new 606 MRIs out of the original dataset.

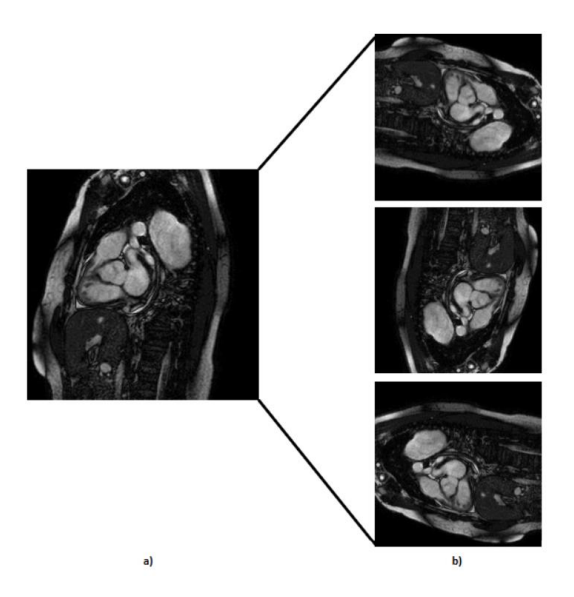


Figure 8 - Representation of the rotation technique applied at the default MRI, where (a) represents the default MRI and (b) represents the MRI with 90, 180, and 270 rotation degrees, respectively.

(2) We executed translation along the x-axis, Figure 9, while meticulously ensuring that the aortic valve remained within the frame, with this we created more 202 MRIs out of the original dataset.

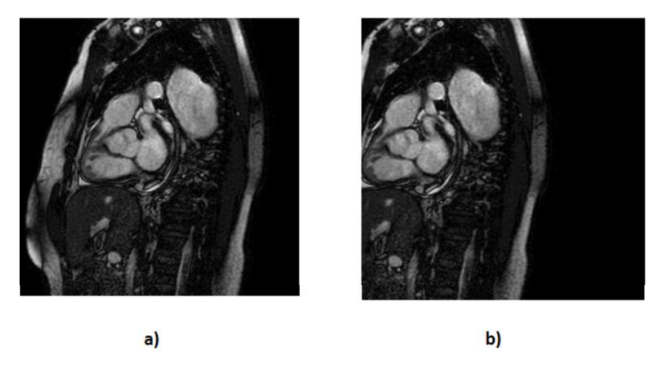


Figure 9 - Representation of the translation technique applied at the default MRI, where (a) represents the default MRI and (b) represents vertical translation.

(3) We have applied horizontal flipping, Figure 10, further diversifying our dataset by creating mirrored counterparts of existing images. With this process we created more 202 MRIs and also introduced new perspectives for our models to learn from.

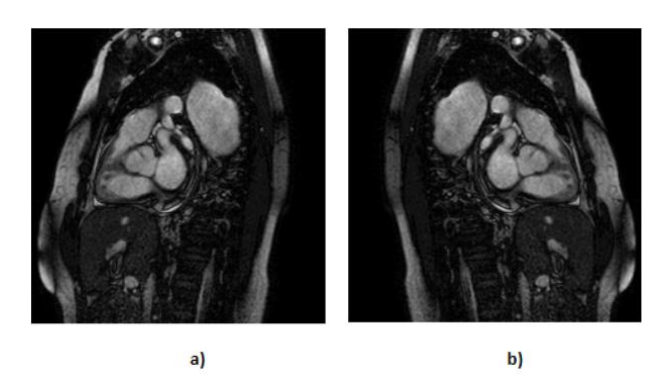


Figure 10 - Representation of the flip technique applied at the default MRI, where (a) represents the default MRI and (b) represents the flipped MRIs.

(4) Recognizing by the cardiology specialist the occasional presence of underexposed images, we addressed this issue by enhancing brightness in the images, Figure 11. By compensating for the darker images, we ensured that our dataset covered a wider spectrum of lighting conditions, thus reinforcing the adaptability of our models. With this technique we created more 404 MRIs.

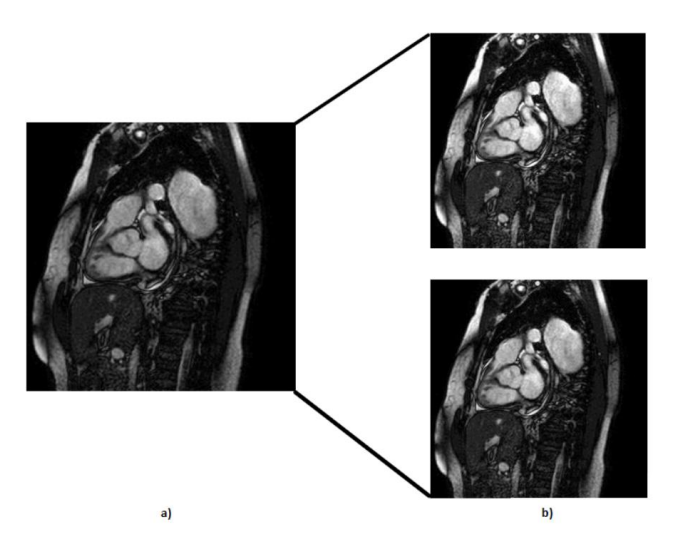


Figure 11 - Representation of the brightness technique applied at the default MRI, where (a) represents the default MRI and (b) represents the brighter MRIs.

In summary, these data augmentation strategies helped us overcome the limitations imposed by our initial dataset size. By injecting diversity, variability, and completeness into our dataset, we equipped our models with the necessary ingredients to extract nuanced insights, leading to the refinement and improvement of our research outcomes. With this our dataset for each test got:

- (1) 1st test (without Data Augmentation) 202 images, 91 with calcification and 111 without calcification.
- (2) 2nd test (Rotation, Flip and Translation) 1,212 images, 546 with calcification and 666 without calcification.
- (3) 3rd test (Rotation, Flip, Translation and Brightness) 1,616 pictures, 729 with calcification and 888 without calcification.

The entire data preparation process is summarized in Figure 12.

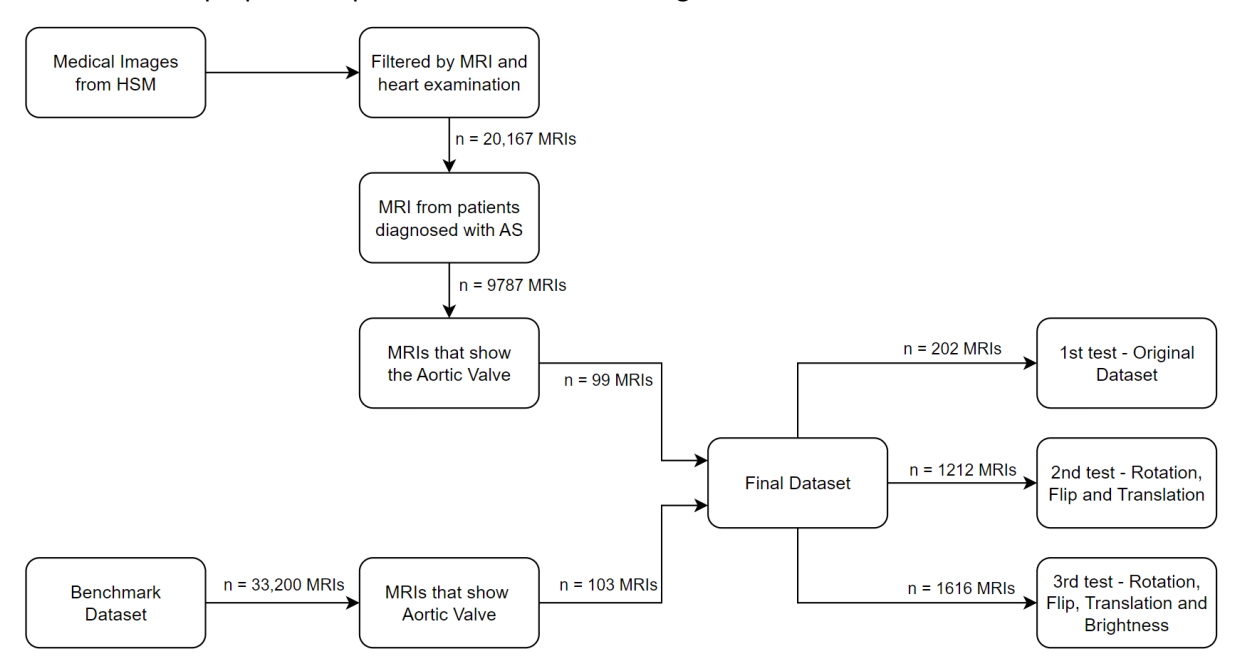


Figure 12 - Summarization of the data preparation.

3.3 Modelling

In this sub-chapter, we strike at the core of our research, utilizing CNNs for the classification of MRI scans to detect AS.

CNNs are an important component of deep learning, achieving excellence in image-related tasks due to their innate ability to learn hierarchical features from input data [56]. Their distinctive architecture, characterized by convolutional layers applying filters to input data for automatic feature extraction, makes CNNs highly effective in capturing subtle patterns and feature hierarchies. These attributes render them ideal for intricate image classification tasks like AS detection.

For this experiment, we developed and implemented our own CNN model, conducting multiple experiments to achieve optimal results. To address the inherent limitations of our dataset, stemming from both the results obtained and the restricted dataset access, we employed CNNs in conjunction with transfer learning and data augmentation techniques. As demonstrated in the literature review, and by previous studies, transfer learning is often employed to overcome the challenge of limited labeled data in medical image analysis [57]. In our experiment, we utilized pretrained weights from the publicly available 'ImageNet' dataset [58], which covers a wide range of classes. Specifically, we selected the VGG16 [59], ResNet-50 [60], and Xception [61] models based on established research findings [45,60–62]. In a comprehensive review [62], the authors identified these models as suitable for medical image classification. Additionally, other works, including [63], [64], highlight ResNet50 as a suitable algorithm for MRI classification, and [63] not only confirms the efficacy of ResNet50 but also demonstrates the implementation of VGG16.

All the pre-trained models utilized in our investigation required robust feature extraction to distinguish various regions within MRI scans and identify the aortic valve for precise classification. To meet this objective, we augmented each model with four additional dense layers, simplifying training with our data. These adjustments produced promising results, aligning closely with the specific feature requirements of our study.

Nonetheless, certain refinements were deemed necessary to fully use the potential of these models. Given our binary classification task, the model's output layer featured a single neuron with sigmoid activation. We implemented a five-fold cross-validation strategy to enhance model performance and mitigate overfitting concerns. This process involved randomizing the dataset and training the model five times, ensuring robustness and generalization.

Additionally, we explored the use of fine-tuning, as suggested in the literature review. This technique involves retraining the last layers of the model while keeping the upper layers untrainable, harnessing the pre-trained model's knowledge and feature extraction capabilities to efficiently adapt it to our specific task-classifying aortic stenosis. This not only enhances model performance but also optimizes time and computing resources.

For modelling, we have splitted our data in the proportion of 80% for training and 20% test to train and test the models [65], see Figure 13.

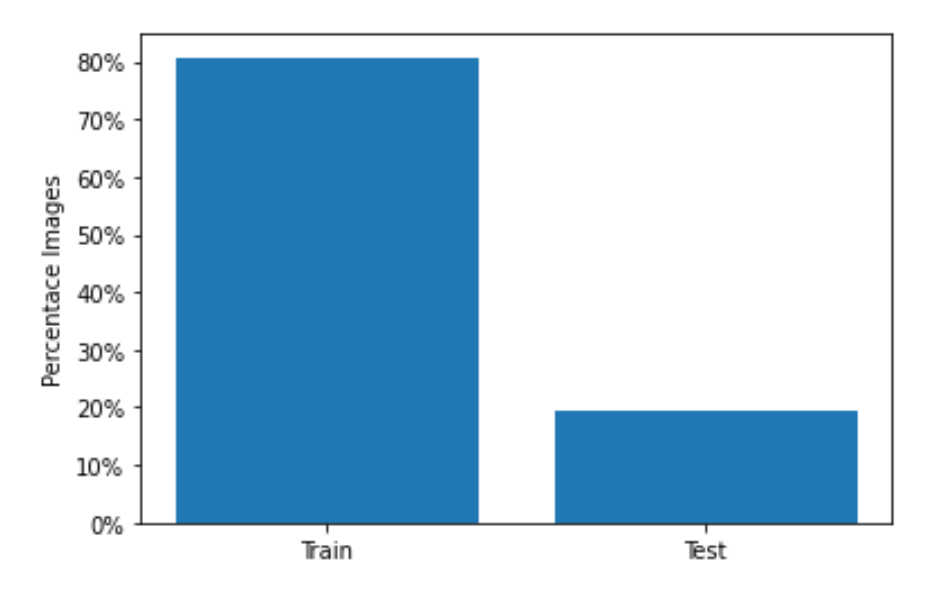


Figure 13 - Percentage of test and train images

We hoped to leverage the full power of CNN models in our pursuit of precise AS categorization by incorporating these adjustments and fine-tuning procedures.

CHAPTER 4 - Evaluation and Discussion

In this chapter, we evaluate and compare the results and performance of the three CNN models that were used in this research work, using the dataset created with images from Hospital Santa Maria and from the benchmark dataset [55].

For the evaluation of the models and Data Augmentation techniques, three tests with different types of image augmentation were conducted. The models in each test remained unmodified and were defined with the following parameters:

- Input shape was defined based on the architecture of each model, where on VGG16 and ResNet50 was (224, 224, 3) and for the Xception was (299, 299, 3).
- The number of batches was set to 32 based on the following formula (1), where N is the number of samples divided with B the batch size multiplied by E number of epochs [66].

Number of Batches =
$$\frac{N}{B*E}$$
 (1)

• The number of epochs was set to 30 based on a considerable number of tests. Initially, we began with 10 epochs, but through experimentation, we observed that the model could be effectively trained for additional epochs without compromising the results. As we increased the number of epochs, we found that not a single test could reach 30 epochs. This was due to the implementation of the early stopping function, indicating that the models were reaching their full capacity. Our early stopping function was defined with a 'patience' parameter set to 4. This means that if, during training, we didn't see better results for four consecutive epochs, the model would stop. This approach was implemented to reduce overfitting while preserving model performance, ultimately saving both time and computational resources.

As previously mentioned, the model parameters remained consistent across all tests. We employed a progressive data augmentation approach, where each test included all the augmentation techniques from the previous test. Consequently, the number of images increased with each test due to the incremental application of these techniques. This approach allowed us to systematically explore the impact of various augmentation methods on our model's performance.

- (1) The first test was without Data Augmentation with 202 MRIs, 91 with calcification and 111 without calcification.
- (2) The second test we applied Flip, Rotation and Translation techniques, ending up with 1,212 MRIs, 546 with calcification and 666 without calcification.

(3) In the third and final test, we added images to the dataset created in the second test using an extra technique known as brightness. The collection now has 1,616 MRIs, 729 with calcification and 888 without calcification.

As we work with MRI classification, we seek to reduce the amount of false negatives (FNs) in order to mitigate patient harm, delayed diagnosis and treatment, and legal and ethical consequences for medical professionals and healthcare institutions if a FN diagnosis harms a patient [67]. So, the Recall measure is the one with the most weight when evaluating different models and data augmentation strategies. The remaining performance metrics serve as supplementary criteria, poised to serve as tiebreakers in cases where models exhibit similar recall rates.

At the outset of this research study, we developed and implemented our custom CNN model. Due to the limited number of images, our optimal architecture consisted of two convolutional layers, each paired with a pooling layer and a hidden layer with 256 neurons, complemented by a dropout layer of 0.3, as depicted on Figure 14. While we experimented with different architectures, including variations in the number of neurons and an additional hidden layer, the chosen architecture consistently yielded superior results. Attempts to increase model complexity led to decreased performance, highlighting the importance of a simpler architecture for better generalization on the test set.

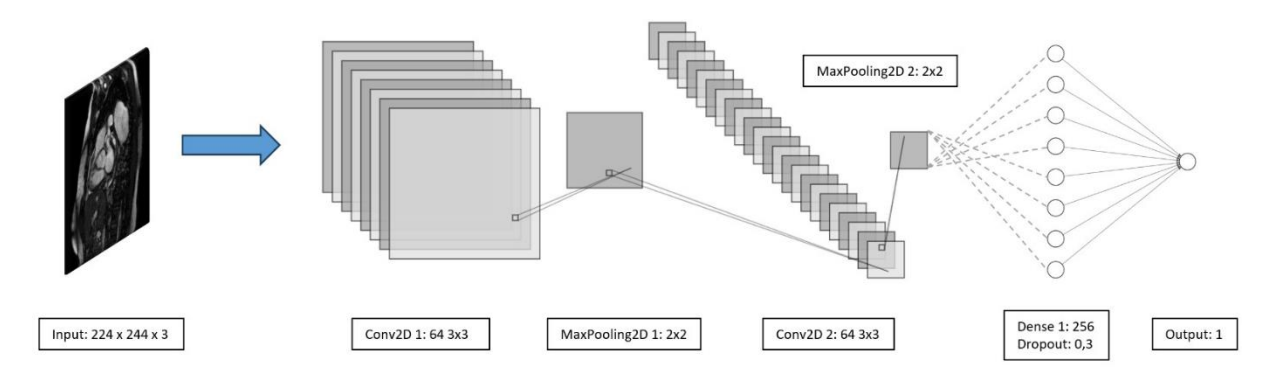


Figure 14 - Developed CNN architecture.

We conducted tests on this model, employing the three different data augmentation techniques mentioned earlier. The results of these tests are detailed in Table 3.

Tabela 3 - Results of the custom CNN model with the different datasets.

Test	Accuracy	Recall	Precision	F1-Score
1. Original Dataset	0.77	0.77	0.77	0.77
2. Rotation, Flip, and Translation	0.78	0.78	0.78	0.78
3. Rotation, Flip, Translation, and Brightness	0.81	0.81	0.81	0.81

Table 3 illustrates that the third test yielded the best results, underscoring the positive impact of data augmentation on the model. This outcome also emphasizes the importance of a larger dataset to enhance performance. Figure 10 depicts the performances of the third test for both training and testing. It is noticeable that, while the model continues to learn and achieves seemingly perfect results (100%) on the training set, this level of results does not extend to the testing set. This discrepancy suggests that our model struggles to generalize its training insights to the testing set. The test set is the most important since it simulates real-world implementation conditions.

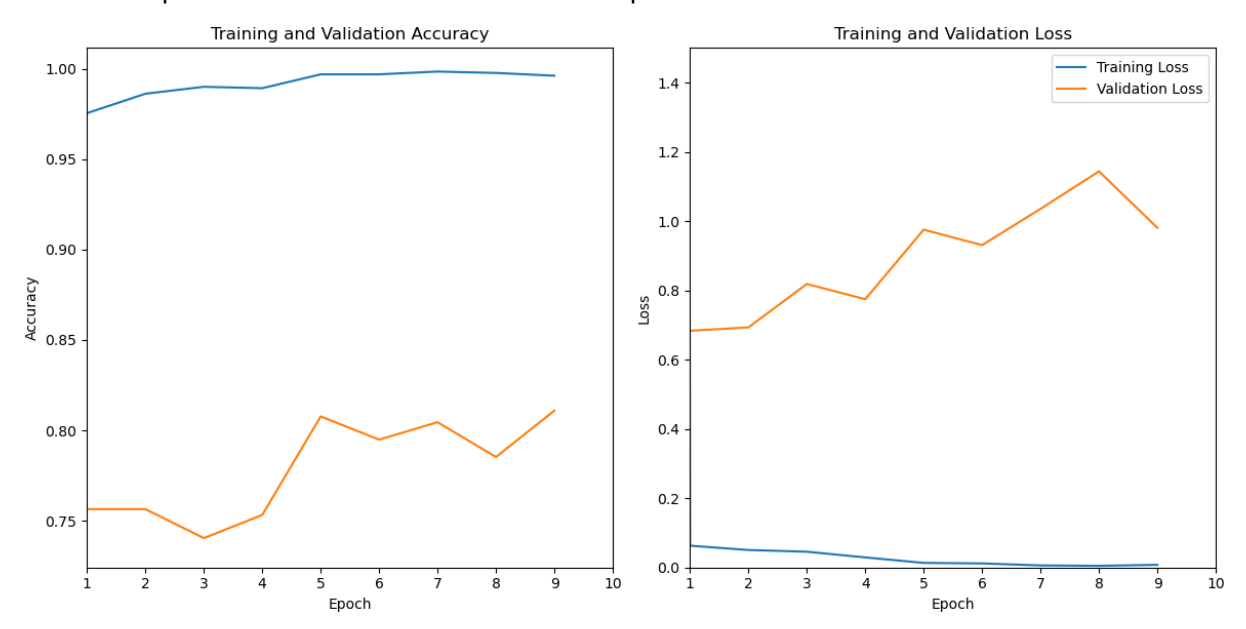


Figure 15 - Model performance: training vs testing.

In light of the observed challenges in model generalization, particularly in real-world testing conditions, we recognized the need for a more robust and adaptable approach. Given the limitations revealed by our initial results, where the algorithm struggled to generalize effectively, we turned our attention to the implementation of transfer learning. This strategic shift aims to take advantage of the pre-trained models and their extensive knowledge to enhance our model's ability to handle diverse and challenging scenarios as we seek to overcome the limitations encountered in the initial model evaluations. As a pivotal step toward improving generalization and model robustness, the incorporation of transfer learning brings a fresh perspective to our approach in addressing the intricacies of aortic stenosis classification in MRI scans.

Consistent with the data augmentation tests outlined in the experiment in Table 3, we have applied these tests to the selected pre-trained models.

The initial test with the original dataset of 202 images revealed distinct performance patterns among the models. VGG16 demonstrated moderate performance, while fine-tuning notably improved its recall, precision, and F1-score. ResNet50 exhibited decent performance, and fine-tuning led to

significant enhancements across all metrics. Xception delivered overall good performance, although fine-tuning showed a decrease in all metrics.

Introducing data augmentation techniques (rotation, flip, and translation) with an expanded dataset of 1212 images resulted in notable improvements. VGG16 consistently showed enhanced performance in all metrics. VGG16 with fine-tuning maintained generally good performance, experiencing a slight decrease in recall. ResNet50 consistently achieved high performance across all metrics, with fine-tuning demonstrating excellent results. Xception consistently displayed good performance, and fine-tuning showed a decrease in recall while maintaining good precision and F1-score.

Extending data augmentation to include brightness, with a larger dataset of 1616 images, further refined model performance. VGG16 demonstrated excellent performance across all metrics. VGG16 with fine-tuning exhibited good precision and F1-score, with a slight decrease in recall. ResNet50 maintained good precision and F1-score, with a slight decrease in recall. ResNet50 with fine-tuning demonstrated excellent performance, with a slight decrease in recall. Xception consistently delivered good performance, and fine-tuning resulted in a decrease in recall while maintaining good precision and F1-score.

From these tests, and as summarized in Table 4, data augmentation significantly contributed to enhancing model performance, while fine-tuning generally improved the results. VGG16 and ResNet50 consistently performed well, offering robust performance. Xception, although displaying good performance, exhibited more variability across the tests. The choice of a model may depend on specific study goals, emphasizing the trade-offs between precision and recall.

Table 4 - Results of the models with different Datasets

Test	Models	Recall	Precision	F1-Score		
1. Original Dataset	VGG16	0.5	0.5	0.5		
	VGG16-FT	0.75	0.88	0.88		
	ResNet50	0.6	0.86	0.86		
	ResNet50-FT	0.8	0.94	0.94		
	Xception	0.85	0.85	0.85		
	Xception-FT	0.546	0.586	0.586		
2. Rotation, Flip, and Translation	VGG16	0.9	0.92	0.92		
	VGG16-FT	0.85	0.96	0.96		
	ResNet50	0.88	0.97	0.97		
	ResNet50-FT	0.93	1	1		
	Xception	0.86	0.86	0.86		
	Xception-FT	0.73	0.87	0.87		
3. Rotation, Flip, Translation and Brightness	VGG16	0.95	0.96	0.96		
	VGG16-FT	0.85	0.98	0.98		
	ResNet50	0.82	0.95	0.95		
	ResNet50-FT	0.89	0.96	0.96		
	Xception	0.86	0.86	0.86		
	Xception-FT	0.64	0.87	0.74		

CHAPTER 5 – Conclusions

In conclusion, we have successfully answered the purposed RQ, achieving its primary objectives, which were implemented, and we tested the best CNN model combined with computer vision techniques for the classification of aortic diseases from MRI data. The model's ability to accurately classify MRI images into categories representing the presence or absence of aortic diseases has been demonstrated, with promising results regarding recall and precision.

As highlighted in the literature review, the application of AI for MRI classification has been relatively scarce. While this presented challenges due to the limited prior knowledge and references, it also unveiled a significant research gap.

Because we did not have a dataset, a great deal of time was invested to create one; this made us deflect our attention to the main RQ in a way that we could not implement more techniques.

Despite the limited number of images, the results of this study are promising. We achieved a recall of 81% with a model specifically developed for this problem, utilizing data augmentation without the incorporation of transfer learning. Having a noticeable overfitting problem in this model, we used pre-trained models, where we tested them with three data augmentation techniques. We can see that, just by employing rotation, flip, and translation techniques (used in the second test), the results improved by 8%, and, with the addition of another data augmentation technique used in the third test, the results improved by 2%, where, in each test, the dataset is also augmenting its size. As a result, the VGG16 model used with the dataset of the third test is the best in detecting AS in MRI scans, with 95% recall and 96% precision.

The outcomes of this study not only advance the field of medical image analysis but also offer practical implications for healthcare. The CNN model combined with the computer vision techniques used has the potential to be a significant tool for radiologists and clinicians in their daily practice, helping to achieve more sensitive, precise, and quick aortic disease diagnosis. As we can see from the results achieved, this application of computer vision and artificial intelligence can reduce the workload of radiologists and clinicians.

Additionally, it highlights the greater potential of computer vision and artificial intelligence to transform healthcare and improve patient outcomes.

In conclusion, this study represents a significant step forward in the attempt to harness the potential of computer vision for identifying and managing aortic diseases, providing hope for more future effective and efficient healthcare procedures.

5.1 Future Work

For future research, further improvements and iterations to the work would be beneficial.

As pointed in this thesis our dataset was very limited and not versatile because of the lack of images with different perspectives, so an improved dataset needs to be the focus. The next dataset should incorporate a greater diversity of images from AS, thereby fortifying the model's ability to deliver precise and reliable disease diagnoses. By exposing the model to a wider spectrum of images, we intend to elevate its diagnostic sensitivity and the trustworthiness of its outcomes.

The application of Image Segmentation and object detection to identify the aortic valve (ROI) techniques can refine our model's diagnostic proficiency. The purpose of this addition is to enable precise localization and identification of pathological regions within medical images. This strategic enhancement promises to elevate the diagnostic precision and furnish clinicians with invaluable insights.

Finally, introducing severity assessment will significantly improve patient care and clinical decision-making. This implementation will empower our model to evaluate the stage and severity of diseases. As a result, the models will distinguish advanced disease stages, reducing even more the medical workload.

References

- [1] 'Cardiovascular diseases (CVDs)'. Accessed: Oct. 06, 2023. [Online]. Available: https://www.who.int/news-room/fact-sheets/detail/cardiovascular-diseases-(cvds)
- [2] T. Gaziano, K. S. Reddy, F. Paccaud, S. Horton, and V. Chaturvedi, 'Cardiovascular Disease', in *Disease Control Priorities in Developing Countries*, 2nd ed., D. T. Jamison, J. G. Breman, A. R. Measham, G. Alleyne, M. Claeson, D. B. Evans, P. Jha, A. Mills, and P. Musgrove, Eds., Washington (DC): The International Bank for Reconstruction and Development / The World Bank, 2006. Accessed: Oct. 05, 2023. [Online]. Available: http://www.ncbi.nlm.nih.gov/books/NBK11767/
- [3] J. S. Da Silveira 'Quantification of aortic stenosis diagnostic parameters: Comparison of fast 3 direction and 1 direction phase contrast CMR and transthoracic echocardiography', *J. Cardiovasc. Magn. Reson.*, vol. 19, no. 1, 2017, doi: 10.1186/s12968-017-0339-5.
- [4] C. Zhang, J. Liu, and S. Qin, 'Prognostic value of cardiac magnetic resonance in patients with aortic stenosis: A systematic review and meta-analysis', *PLoS ONE*, vol. 17, no. 2 February, 2022, doi: 10.1371/journal.pone.0263378.
- [5] C. Bucciarelli-Ducci, N. Ajmone-Marsan, M. Di Carli, and E. Nicol, 'The year in cardiovascular medicine 2021: Imaging', *Eur. Heart J.*, vol. 43, no. 13, pp. 1288–1295, 2022.
- [6] 'Level of the SARS-CoV-2 receptor ACE2 activity is highly elevated in old-aged patients with aortic stenosis: implications for ACE2 as a biomarker for the severity of COVID-19 PMC'. Accessed: Dec. 01, 2022. [Online]. Available: https://www.ncbi.nlm.nih.gov/pmc/articles/PMC7815502/
- [7] R. 'Artificial Intelligence Enabled Fully Automated CMR Function Quantification for Optimized Risk Stratification in Patients Undergoing Transcatheter Aortic Valve Replacement', *J. Intervent. Cardiol.*, vol. 2022, Apr. 2022, doi: 10.1155/2022/1368878.
- [8] H. Chen, D. Ouyang, T. Baykaner, F. Jamal, P. Cheng, and J.-W. Rhee, 'Artificial intelligence applications in cardio-oncology: Leveraging high dimensional cardiovascular data', *Front. Cardiovasc. Med.*, vol. 9, 2022, [Online]. Available: https://www.scopus.com/inward/record.uri?eid=2-s2.0-85135614770&doi=10.3389%2ffcvm.2022.941148&partnerID=40&md5=b183a520254bcbddd380c7cd6e596f7
- [9] P. T. Lauzier, R. Avram, D. Dey, P. Slomka, J. Afilalo, and B. J. W. Chow, 'The Evolving Role of Artificial Intelligence in Cardiac Image Analysis', *Can. J. Cardiol.*, vol. 38, no. 2, pp. 214–224, 2022.
- [10] M. E. Nyström, J. Karltun, C. Keller, and B. Andersson Gäre, 'Collaborative and partnership research for improvement of health and social services: researcher's experiences from 20 projects', *Health Res. Policy Syst.*, vol. 16, no. 1, p. 46, May 2018, doi: 10.1186/s12961-018-0322-0.
- [11] A. Dåderman and S. Rosander, 'Evaluating Frameworks for Implementing Machine Learning in Signal Processing: A Comparative Study of CRISP-DM, SEMMA and KDD', Student thesis, 2018. Accessed: Sep. 25, 2018. [Online]. Available: http://urn.kb.se/resolve?urn=urn:nbn:se:kth:diva-235408
 - [12] R. Wirth and J. Hipp, 'CRISP-DM: Towards a Standard Process Model for Data Mining'.
- [13] D. Moher, A. Liberati, J. Tetzlaff, D. G. Altman, and for the PRISMA Group, 'Preferred reporting items for systematic reviews and meta-analyses: the PRISMA statement', *BMJ*, vol. 339, no. jul21 1, pp. b2535–b2535, Jul. 2009, doi: 10.1136/bmj.b2535.
- [14] F. Catapano '4D flow imaging of the thoracic aorta: is there an added clinical value?', *Cardiovasc. Diagn. Ther.*, vol. 10, no. 4, pp. 1068–1089, 2020, doi: 10.21037/cdt-20-452.
- [15] H. SAKLY, M. SAID, S. RADHOUANE, and M. TAGINA, 'Medical decision making for 5D cardiac model: Template matching technique and simulation of the fifth dimension', *Comput. Methods Programs Biomed.*, vol. 191, 2020, doi: 10.1016/j.cmpb.2020.105382.
- [16] M. K. 'Motion-corrected imaging of the aortic valve with 18F-NaF PET/CT and PET/MRI: A feasibility study', *J. Nucl. Med.*, vol. 58, no. 11, pp. 1811–1814, 2017, doi: 10.2967/jnumed.117.194597.
- [17] A. B. Vadher, M. Shaw, N. N. Pandey, A. Sharma, and S. Kumar, 'Stenotic lesions of pulmonary arteries: imaging evaluation using multidetector computed tomography angiography', *Clin. Imaging*, vol. 69, pp. 17–26, 2021, doi: 10.1016/j.clinimag.2020.06.036.
- [18] G. Battineni, M. A. Hossain, N. Chintalapudi, and F. Amenta, 'A Survey on the Role of Artificial Intelligence in Biobanking Studies', *Diagnostics*, vol. 12, no. 5, 2022, [Online]. Available: https://www.scopus.com/inward/record.uri?eid=2-s2.0-
- 85130298335&doi=10.3390%2fdiagnostics12051179&partnerID=40&md5=00a43825d7b0f8cd33cf1ae91e032d
- [19] D. H. Yang, 'Application of artificial intelligence to cardiovascular computed tomography', *Korean J. Radiol.*, vol. 22, pp. 1–12, 2021.

- [20] J. Garcia, A. J. Barker, J. D. Collins, J. C. Carr, and M. Markl, 'Volumetric quantification of absolute local normalized helicity in patients with bicuspid aortic valve and aortic dilatation', *Magn. Reson. Med.*, vol. 78, no. 2, pp. 689–701, 2017, doi: 10.1002/mrm.26387.
- [21] J. Brüning, F. Hellmeier, P. Yevtushenko, T. Kühne, and L. Goubergrits, 'Uncertainty Quantification for Non-invasive Assessment of Pressure Drop Across a Coarctation of the Aorta Using CFD', *Cardiovasc. Eng. Technol.*, vol. 9, no. 4, pp. 582–596, 2018, doi: 10.1007/s13239-018-00381-3.
- [22] N. P. 'Comprehensive assessment of cardiovascular structure and function and disease risk in middle-aged ultra-endurance athletes', *Atherosclerosis*, vol. 320, pp. 105–111, 2021, doi: 10.1016/j.atherosclerosis.2020.11.030.
- [23] B. Jiang, N. Guo, Y. Ge, L. Zhang, M. Oudkerk, and X. Xie, 'Development and application of artificial intelligence in cardiac imaging', *Br. J. Radiol.*, vol. 93, no. 1113, 2020, [Online]. Available: https://www.scopus.com/inward/record.uri?eid=2-s2.0-
- 85089768466&doi=10.1259%2fbjr.20190812&partnerID=40&md5=af32929cc8f03986598c65c50939994e
- [24] F. E. 'Multi-parametric approach to predict prosthetic valve size using CMR and clinical data: insights from SAVR', *Int. J. Cardiovasc. Imaging*, vol. 37, no. 7, pp. 2269–2276, 2021, doi: 10.1007/s10554-021-02203-5.
- [25] L. Hahn, K. Baeumler, and A. Hsiao, 'Artificial intelligence and machine learning in aortic disease', *Curr. Opin. Cardiol.*, vol. 36, no. 6, pp. 695–703, Nov. 2021, doi: 10.1097/HCO.0000000000000003.
- [26] P. Rudzinski 'CT in Transcatheter-delivered Treatment of Valvular Heart Disease', *RADIOLOGY*, vol. 304, no. 1, pp. 4–17, Jul. 2022, doi: 10.1148/radiol.210567.
- 'Clinical recommendations for cardiovascular magnetic resonance mapping of T1, T2, T2 and extracellular volume: A consensus statement by the Society for Cardiovascular Magnetic Resonance (SCMR) endorsed by the European Association for Cardiovascular Imaging (EACVI)', *J. Cardiovasc. Magn. Reson.*, vol. 19, no. 1, 2017, doi: 10.1186/s12968-017-0389-8.
- [28] T. Higashikawa, Y. Ichikawa, M. Ishida, K. Kitagawa, T. Hirano, and H. Sakuma, 'Assessment of coronary flow velocity reserve with phase-contrast cine magnetic resonance imaging in patients with heavy coronary calcification', *Int. J. Cardiovasc. Imaging*, vol. 35, no. 5, pp. 897–905, 2019, doi: 10.1007/s10554-019-01531-x.
- [29] P. G. Peterson, M. Berge, J. P. Lichtenberger III, M. N. Hood, and V. B. Ho, 'Cardiac Imaging Modalities and Appropriate Use', *Prim. Care Clin. Off. Pract.*, vol. 45, no. 1, pp. 155–168, 2018, doi: 10.1016/j.pop.2017.10.006.
- [30] L. 'Diagnostic Performance of Fully Automated Pixel-Wise Quantitative Myocardial Perfusion Imaging by Cardiovascular Magnetic Resonance', *JACC-Cardiovasc. IMAGING*, vol. 11, no. 5, pp. 697–707, May 2018, doi: 10.1016/j.jcmg.2018.01.005.
- [31] T. H. Oechtering, G. S. Roberts, N. Panagiotopoulos, O. Wieben, A. Roldán-Alzate, and S. B. Reeder, 'Abdominal applications of quantitative 4D flow MRI', *Abdom. Radiol.*, vol. 47, no. 9, pp. 3229–3250, 2022, doi: 10.1007/s00261-021-03352-w.
- [32] F. Sagmeister 'Extent of size, shape and systolic variability of the left ventricular outflow tract in aortic stenosis determined by phase-contrast MRI', *Magn. Reson. Imaging*, vol. 45, pp. 58–65, 2018, doi: 10.1016/j.mri.2017.09.002.
- 'Pressure drop mapping using 4D flow MRI in patients with bicuspid aortic valve disease: A novel marker of valvular obstruction', *Magn. Reson. Imaging*, vol. 65, pp. 175–182, 2020, doi: 10.1016/j.mri.2019.11.011.
- [37] J. M. Tarkin, A. Ä †orović, C. Wall, D. Gopalan, and J. H. F. Rudd, 'Positron emission tomography imaging in cardiovascular disease', *Heart*, 2020, doi: 10.1136/heartjnl-2019-315183.
- [38] H. Ha, J.-P. E. Kvitting, P. Dyverfeldt, and T. Ebbers, 'Validation of pressure drop assessment using 4D flow MRI-based turbulence production in various shapes of aortic stenoses', *Magn. Reson. Med.*, vol. 81, no. 2, pp. 893–906, 2019, doi: 10.1002/mrm.27437.
- [39] S. Celi, N. Martini, L. E. Pastormerlo, V. Positano, and S. Berti, 'Multimodality imaging for interventional cardiology', *Curr. Pharm. Des.*, vol. 23, no. 22, pp. 3285–3300, 2017, doi: 10.2174/1381612823666170704171702.
- [40] S. Chandrasekhar, G. Laxminarayana, and Y. Chakrapani, 'Novel hybrid segmentation techniques for cardiac image processing in remote health care monitoring systems', *J. Med. Imaging Health Inform.*, vol. 7, no. 6, pp. 1153–1159, 2017, doi: 10.1166/jmihi.2017.2202.
- [41] Y.-C. Chen, X.-E. Wei, J. Lu, R.-H. Qiao, X.-F. Shen, and Y.-H. Li, 'Correlation between intracranial arterial calcification and imaging of cerebral small vessel disease', *Front. Neurol.*, vol. 10, no. MAY, 2019, doi: 10.3389/fneur.2019.00426.

- [42] Y. Luo, L. Xu, and L. Qi, 'A cascaded FC-DenseNet and level set method (FCDL) for fully automatic segmentation of the right ventricle in cardiac MRI', *Med. Biol. Eng. Comput.*, vol. 59, no. 3, pp. 561–574, 2021, doi: 10.1007/s11517-020-02305-7.
- [43] D. Qiu, L. Peng, D. N. Ghista, and K. K. L. Wong, 'Left Atrial Remodeling Mechanisms Associated with Atrial Fibrillation', *Cardiovasc. Eng. Technol.*, vol. 12, no. 3, pp. 361–372, 2021, doi: 10.1007/s13239-021-00527-w.
- [44] S. 'Lenticulostriate artery combined with neuroimaging markers of cerebral small vessel disease differentiate the pathogenesis of recent subcortical infarction', *J. Cereb. Blood Flow Metab.*, vol. 41, no. 8, pp. 2105–2115, 2021, doi: 10.1177/0271678X21992622.
- 'Classification of cardioembolic stroke based on a deep neural network using chest radiographs', *EBioMedicine*, vol. 69, 2021, [Online]. Available: https://www.scopus.com/inward/record.uri?eid=2-s2.0-85109019844&doi=10.1016%2fj.ebiom.2021.103466&partnerID=40&md5=d008ad55e824a3019259349cf2891 8f1
- [46] N. Kagiyama, S. Shrestha, P. D. Farjo, and P. P. Sengupta, 'Artificial intelligence: practical primer for clinical research in cardiovascular disease', *J. Am. Heart Assoc.*, vol. 8, no. 17, Art. no. 17, 2019, doi: 10.1161/JAHA.119.012788.
- [47] A. Pasteur-Rousseau and J.-F. Paul, 'Artificial Intelligence and teleradiology in cardiovascular imaging by CT-Scan and MRI', *Ann. Cardiol. Angeiol. (Paris)*, vol. 70, no. 5, Art. no. 5, 2021, doi: 10.1016/j.ancard.2021.08.001.
- [48] M. V. 'Position statement on diagnosis and treatment of cardiac amyloidosis 2021', *Arq. Bras. Cardiol.*, vol. 117, no. 3, Art. no. 3, 2021, doi: 10.36660/abc.20210718.
- [49] Z. Zahisham, C. P. Lee, and K. M. Lim, 'Food Recognition with ResNet-50', in 2020 IEEE 2nd International Conference on Artificial Intelligence in Engineering and Technology (IICAIET), Sep. 2020, pp. 1–5. doi: 10.1109/IICAIET49801.2020.9257825.
- [50] R. J. Gropler, 'In This Issue of the Journal', *Circ. Cardiovasc. Imaging*, vol. 12, no. 9, Art. no. 9, 2019, doi: 10.1161/CIRCIMAGING.119.009851.
- [51] R. Nath, S. Callahan, N. Singam, M. Stoddard, A. Amini, and IEEE, 'Accelerated Phase Contrast Magnetic Resonance Imaging via Deep Learning', presented at the 2020 IEEE 17TH INTERNATIONAL SYMPOSIUM ON BIOMEDICAL IMAGING (ISBI 2020), 2020, pp. 834–838.
- [52] 'Detalhes do Projeto Ciência-IUL ISCTE-IUL'. Accessed: Oct. 06, 2023. [Online]. Available: https://ciencia.iscte-iul.pt/projects/aplicacoes-moveis-baseadas-em-inteligencia-artificial-para-resposta-de-saude-publica/1567
- [53] R. Andorno, 'The Oviedo Convention: A European Legal Framework at the Intersection of Human Rights and Health Law', vol. 2, no. 4, pp. 133–143, 2005, doi: 10.1515/jibl.2005.2.4.133.
- [54] D. R. Varma, 'Managing DICOM images: Tips and tricks for the radiologist', *Indian J. Radiol. Imaging*, vol. 22, no. 01, pp. 4–13, Jan. 2012, doi: 10.4103/0971-3026.95396.
- [55] F. Khozeimeh 'RF-CNN-F: random forest with convolutional neural network features for coronary artery disease diagnosis based on cardiac magnetic resonance', *Sci. Rep.*, vol. 12, no. 1, p. 11178, Jul. 2022, doi: 10.1038/s41598-022-15374-5.
- 'Modeling of Reptile Search Algorithm With Deep Learning Approach for Copy Move Image Forgery Detection', *IEEE Access*, vol. 11, pp. 87297–87304, 2023, doi: 10.1109/ACCESS.2023.3304237.
- [57] R. Wang, T. Lei, R. Cui, B. Zhang, H. Meng, and A. K. Nandi, 'Medical image segmentation using deep learning: A survey', *IET Image Process.*, vol. 16, no. 5, pp. 1243–1267, 2022, doi: 10.1049/ipr2.12419.
- [58] J. Deng, W. Dong, R. Socher, L. -J. Li, Kai Li, and Li Fei-Fei, 'ImageNet: A large-scale hierarchical image database', in *2009 IEEE Conference on Computer Vision and Pattern Recognition*, Jun. 2009, pp. 248–255. doi: 10.1109/CVPR.2009.5206848.
- [59] 'A deep learning based convolutional neural network model with VGG16 feature extractor for the detection of Alzheimer Disease using MRI scans', *Meas. Sens.*, vol. 24, p. 100506, Dec. 2022, doi: 10.1016/j.measen.2022.100506.
- [60] D. S, L. Padma Suresh, and A. John, 'A Deep Transfer Learning framework for Multi Class Brain Tumor Classification using MRI', in 2020 2nd International Conference on Advances in Computing, Communication Control and Networking (ICACCCN), Dec. 2020, pp. 283–290. doi: 10.1109/ICACCCN51052.2020.9362908.
- [61] B. Gülmez, 'A novel deep neural network model based Xception and genetic algorithm for detection of COVID-19 from X-ray images', *Ann. Oper. Res.*, vol. 328, no. 1, pp. 617–641, Sep. 2023, doi: 10.1007/s10479-022-05151-y.
- [62] H. E. Kim, A. Cosa-Linan, N. Santhanam, M. Jannesari, M. E. Maros, and T. Ganslandt, 'Transfer learning for medical image classification: a literature review', *BMC Med. Imaging*, vol. 22, no. 1, p. 69, Apr. 2022, doi: 10.1186/s12880-022-00793-7.

- [63] S. Mascarenhas and M. Agarwal, 'A comparison between VGG16, VGG19 and ResNet50 architecture frameworks for Image Classification', in 2021 International Conference on Disruptive Technologies for Multi-Disciplinary Research and Applications (CENTCON), Nov. 2021, pp. 96–99. doi: 10.1109/CENTCON52345.2021.9687944.
- [64] Y. 'Deep Learning-based Automatic Diagnosis of Breast Cancer on MRI Using Mask R-CNN for Detection Followed by ResNet50 for Classification', *Spec. Issue Womens Imaging Focus*, vol. 30, pp. S161–S171, Sep. 2023, doi: 10.1016/j.acra.2022.12.038.
- [65] A. Gholamy, V. Kreinovich, and O. Kosheleva, 'Why 70/30 or 80/20 Relation Between Training and Testing Sets: A Pedagogical Explanation', 2018, Accessed: Oct. 06, 2023. [Online]. Available: https://scholarworks.utep.edu/cs_techrep/1209
- [66] 'Calculating The Batch Size In Keras modeladvisor.com'. Accessed: Oct. 12, 2023. [Online]. Available: https://www.modeladvisor.com/calculating-the-batch-size-in-keras/
- [67] C.-H. Chiang, C.-L. Weng, and H.-W. Chiu, 'Automatic classification of medical image modality and anatomical location using convolutional neural network', *PLOS ONE*, vol. 16, no. 6, p. e0253205, Jun. 2021, doi: 10.1371/journal.pone.0253205.